Transactions, SMiRT-25
Charlotte, NC, USA, August 4-9, 2019
Division III

STRESS TEST SEISMIC MOTIONS FOR NUCLEAR INSTALLATIONS

Hexiang Wang[1], Yuan Feng[2], Han Yang[1], Fangbo Wang[3], Boris Jeremić[4,5]

[1] PhD Candidate, University of California, Davis, CA, USA
[2] Research Scientist, TuSimple, San Diego, CA, USA
[3] Assistant Professor, Tianjin University, Tianjin, China
[4] Professor, University of California, Davis, CA, USA
[5] Faculty Scientist, Lawrence Berkeley National Laboratory, Berkeley, CA, USA

ABSTRACT

Presented is a methodology to stress test soil structure interaction (SSI) systems using spatially varying three components (3C) seismic motions. The main idea is to develop seismic motions that excite broadband of frequencies, a range of intensities and incident wave angles, for variation in body and surface waves. In this study, it is acceptable to numerically fail the nuclear installation (NI) system, to develop high accelerations, damage structural components, and push NI system far beyond design states. Insights into possible damages and failure modes give engineers useful information that can lead to improving design of new and retrofitting existing NIs.

The complete 3C seismic motions from inclined plane body waves and surface waves with variation in incident angle, frequency and intensities are developed using wave potential formulation. The 3C seismic excitations are then applied to SSI system by domain reduction method (DRM). Dynamic response of SSI system is simulated through finite element analysis. High frequency stress test motions are obtained analytically using Thompson-Haskell propagator matrix technique. Frequency content is only limited by the mesh size of finite element model of SSI system. Proposed methodology is implemented in the Real ESSI Simulator and is illustrated through stress tests of a deeply embedded small modular reactor (SMR). Different stress test responses of SMR are compared. Suggestions for improved design of NIs are given.

INTRODUCTION

Spatially-varying three component (3C) seismic motions from inclined body waves (P and SV wave) and surface waves have been consistently observed from seismic records (Trifunac et al., 1999, Kozák, 2009, Cucci & Tertulliani, 2011, 2013, Yin et al., 2016). The 3C seismic motions could have significant influences (wave passage effects) on the dynamic response of SSI system, especially in near-fault regions and for structures with large-plan dimension. Differential 3C ground excitations could cause torsional and additional rocking response of SSI system. Unfortunately, in many engineering practices, seismic motion fields are assumed as 1D uniform, vertically propagated shear waves (two horizontal components) and/or compressional wave (vertical component). 1D motion convolution/deconvolution is repeatedly performed in three directions

for three times with programs, for example, SHAKE, to generate uniform 1D motion in three components so-called $3 \times 1C$ seismic motions. (Over-) Simplified $3 \times 1C$ seismic motions can introduce modeling uncertainty into dynamic response of SSI system.

Dynamic SSI under $3C$ seismic excitations has been investigated by many researchers. Analytical solutions to SSI system with incident plane SH wave are derived by Wong & Trifunac (1974), Luco (1976), Liang et al. (2016). Wolf (1989) formulated sub-structure method, where the complicated dynamic SSI problem is decomposed into three sub-problems: Free field motions, foundation scattering and impedance function, and superstructural response. Following that, Impedance functions for several specific foundation shapes (rectangular, hemispherical, etc) and soil profiles have been developed (Wong & Luco, 1985, Crouse et al., 1990, Fu et al., 2017). Todorovska & Trifunac (1992) and Todorovska (1993) studied dynamic SSI under incident P, SV and Rayleigh wave. Effects of site dynamic characteristics on SSI for incident P, SV and SH waves were systematically explored by Liang et al. (2013*b*,*a*). Great research progress has been made over the past several decades. However, because of the complexity of the problem, some simplifications and assumptions are adopted in many existing studies. For example, rigid foundation with specific shape is typically assumed to calculate impedance functions and wave scattering. Simplified ground conditions, e.g., homogeneous half space or single homogeneous soil layer above bedrock tend to be considered. In addition, substructure method is derived based on principal of superposition, which fundamentally limits its application to nonlinear problems.

On the other hand, domain reduction method (DRM) has been originally developed in the field of seismology to study local topography effects (Bielak et al., 2003, Yoshimura et al., 2003). DRM was then adopted to solve earthquake SSI with great success (Jeremić et al., 2009, Abell et al., 2018, Wang et al., 2019). With DRM, a few large scale numerical simulations of SSI under $3C$ seismic excitation have been performed (Jeremić et al., 2013, Wang et al., 2017, Sinha et al., 2017). These large scale numerical simulations can precisely capture irregular structural geometry, ground inhomogeneity, nonlinearity and $3C$ seismic motions in the system. However, it is difficult to interpret simulation results because of simultaneous action of many complex factors (Gičev et al., 2016). The influence mechanisms of $3C$ motions and potentially beneficial or detrimental effects of $3 \times 1C$ simplification on SSI are still poorly understood. Furthermore, due to computational limitations, the valid frequency range of modeled 3C seismic motions is usually only up to several Hertz, which is not sufficient for many critical structures, e.g., NPP.

After 2011 Fukushima nuclear accident, reactor risk and safety assessments ("stress test") were emphasized and carried out on all European Union (EU) power plants (Stress Test Peer Review Board, 2012). The purpose of stress test is to assess how nuclear installations can withstand the consequences of various extreme external events, such as earthquakes, tsunami and floods. Among these, it is important to develop full-spectrum possible seismic motions to stress test the seismic safety of NIs. To this end, this paper first formulated $3C$ seismic motion field in layering ground from oblique incident plane waves with wave potential approach. A wide range of frequencies, incident angles and intensities can be accounted for. Then a deeply embedded small modular reactor (SMR) is stress tested with developed $3C$ seismic excitations. Different dynamic responses of SMR are compared and suggestions for improved design of NIs are given.

STRESS TEST SEISMIC MOTIONS FROM INCIDENT PLANE WAVES

Since the incidence of out-of-plane SH wave is simpler and well studied, here we focus on the incidence of P and SV wave. The wave potential formulations below are general and can be applied to incident SH wave with little modification. According to the Helmholtz decomposition theorem (Arfken & Weber, 1999), the displacement of wave propagation equation in linear elastic media can be expressed with P wave scalar potential ϕ and S wave vector potential $\mathbf{\Psi}$ as shown in equation 1, where ϕ is the curl free part corresponding to volumetric deformation and $\mathbf{\Psi}$ is divergence free part (i.e. $\nabla \cdot \mathbf{\Psi} = 0$) corresponding to deviatoric deformation.

$$\boldsymbol{u} = \nabla\phi + \nabla \times \Psi \tag{1}$$

Considered here is 2D layering ground in XZ plane with layer thickness d_m, density ρ_m, compressional velocity α_m and shear wave velocity β_m ($m = 1, 2, .., n$). n is the total number of layers. Monochromatic in-plane incident waves is considered. The wave angular frequency is w with horizontal phase velocity c. Excitations of multiple frequencies can be Fourier synthesized with monochromatic solutions. The unknown variables for m^{th} layer are simplified into incident P wave potential magnitude $\phi_m^{'}$, reflected P wave potential magnitude $\phi_m^{''}$, incident SV wave potential magnitude $\Psi_m^{'}$ and reflected SV wave potential magnitude $\Psi_m^{''}$. The P and SV wave potential takes the following complex form, where k is the horizontal wave number, equals to w/c. And $cot^{-1}\gamma_{\alpha_m}$ and $cot^{-1}\gamma_{\beta_m}$ are incident and reflected angles for P and SV wave, respectively.

$$\begin{aligned}\phi_m &= [\phi_m^{'} e^{ik(x-\gamma_{\alpha m} z)} + \phi_m^{''} e^{ik(x+\gamma_{\alpha m} z)}] e^{-iwt} \\ \Psi_m &= [\Psi_m^{'} e^{ik(x-\gamma_{\beta m} z)} + \Psi_m^{''} e^{ik(x+\gamma_{\beta m} z)}] e^{-iwt}\end{aligned} \tag{2}$$

The solutions to dilatational wave Δ_m and rotational wave ω_m are presented with wave potentials as follows:

$$\begin{aligned}\phi_m &= -(\frac{\alpha_m}{w})^2 \Delta_m \\ \Psi_m &= 2(\frac{\beta_m}{w})^2 \omega_m\end{aligned} \tag{3}$$

Using the continuity condition of displacement field u_x, u_z and stress field σ_{zz}, τ_{zx} at the ground interfaces, the solution at $(m-1)^{th}$ interface $S^{(m-1)}$ and m^{th} interface $S^{(m)}$ can be expressed with dilatational wave magnitude $(\Delta_m^{'}, \Delta_m^{''})$ and rotational wave magnitude $(\omega_m^{'}, \omega_m^{''})$ of m^{th} layer in following matrix notations(Haskell, 1953), where $S^{(m)}$ is equal to $[\dot{u}_x(z_m = d_m)/c, \dot{u}_z(z_m = d_m)/c, \sigma_{zz}(z_m = d_m), \tau_{zx}(z_m = d_m)]^T$.

$$S^{(m-1)} = \boldsymbol{E_m}[\Delta_m^{''} + \Delta_m^{'}, \Delta_m^{''} - \Delta_m^{'}, \omega_m^{''} - \omega_m^{'}, \omega_m^{''} + \omega_m^{'}]^T \tag{4}$$

$$S^{(m)} = \boldsymbol{D_m}[\Delta_m^{''} + \Delta_m^{'}, \Delta_m^{''} - \Delta_m^{'}, \omega_m^{''} - \omega_m^{'}, \omega_m^{''} + \omega_m^{'}]^T \tag{5}$$

The recurrence relation between $S^{(m)}$ and $S^{(m-1)}$ then can be established as equation 6. Wang et al.

(2019) gives detailed derivation of the propagator matrix D_m, E_m and G_m.

$$S^{(m)} = \boldsymbol{D_m E_m^{-1}} S^{(m-1)} = \boldsymbol{G_m} S^{(m-1)} \tag{6}$$

Recursively applying equation 6 leads to equation 7, which builds the relationship between the upper boundary and lower boundary. Applying following boundary conditions into equation 7: (1) The traction at the ground surface ($z = 0$) is zero (i.e. the third and fourth component of $S^{(0)}$ is 0). (2) At n^{th} layer, the incident in-plane P and SV wave potential magnitude $\phi_n^{'}$ and $\Psi_n^{'}$ are given as K_1 and K_2.

$$\begin{aligned} S^{(0)} &= \boldsymbol{L}[\Delta_n^{''} + \Delta_n^{'}, \Delta_n^{''} - \Delta_n^{'}, \omega_n^{''} - \omega_n^{'}, \omega_n^{''} + \omega_n^{'}]^T \\ \boldsymbol{L} &= (\prod_{i=1}^{n-1} \boldsymbol{G_i})^{-1} \boldsymbol{E_n} \end{aligned} \tag{7}$$

The reflected dilatational wave magnitude and rotational wave magnitude can be solved by equation 8, where $\Delta_n^{'}$ is $-K_1(\omega/\alpha_n)^2$ and $\omega_n^{'}$ is $K_2 w^2/(2\beta_n^2)$.

$$\begin{bmatrix} \Delta_n^{''} \\ \omega_n^{''} \end{bmatrix} = \begin{bmatrix} L_{31} + L_{32} & L_{33} + L_{34} \\ L_{41} + L_{42} & L_{43} + L_{44} \end{bmatrix}^{-1} \begin{bmatrix} (L_{32} - L_{31})\Delta_n^{'} + (L_{33} - L_{34})\omega_n^{'} \\ (L_{42} - L_{41})\Delta_n^{'} + (L_{43} - L_{44})\omega_n^{'} \end{bmatrix} \tag{8}$$

Finally, dilatational wave magnitude Δ and rotational wave magnitudes ω for the rest $n-1$ layers can be traced back with recurrence relation equation 9. The displacement and stress field can be easily computed with solved potential magnitudes of each layer.

$$\begin{bmatrix} \Delta_{m-1}^{''} + \Delta_{m-1}^{'} \\ \Delta_{m-1}^{''} - \Delta_{m-1}^{'} \\ \omega_{m-1}^{''} - \omega_{m-1}^{'} \\ \omega_{m-1}^{''} + \omega_{m-1}^{'} \end{bmatrix} = \boldsymbol{D_{m-1}^{-1} E_m} \begin{bmatrix} \Delta_m^{''} + \Delta_m^{'} \\ \Delta_m^{''} - \Delta_m^{'} \\ \omega_m^{''} - \omega_m^{'} \\ \omega_m^{''} + \omega_m^{'} \end{bmatrix} \tag{9}$$

WAVE POTENTIAL - DOMAIN REDUCTION METHOD FOR ESSI WITH 3C MOTIONS

The methodology of wave potential - domain reduction method (WP-DRM) consists of three components: First, free field $3C$ seismic motions from oblique incident plane waves are solved following the aforementioned wave potential formulation. Then dynamically consistent effective earthquake forces are computed from free field response and applied at the DRM layer in the finite element model of SSI system (Bielak et al., 2003). Finally, dynamic response of SSI system are simulated with FEM.

Compared with conventional substructure method, WP-DRM has the following advantages: (1) Substructure method requires to solve not only the free field motions but also wave scattering from the foundation and impedance function for foundation and ground system. However, both wave scattering and foundation impedance functions are themselves very difficult issues. Only several specific shapes (hemispherical, elliptic, etc.) of foundation embedded in simplified ground conditions have been well studied (Fu et al., 2017). In contrast, WP-DRM requires only free field motions. The wave scattering and dynamic SSI under $3C$ seismic excitations are directly simulated through time domain FEM analysis under effective earthquake forces. (2)

Table 1: Layering properties for free field verification

Layer ID	Thickness d [m]	density ρ $[kg/m^3]$	V_s $[m/s]$	V_p $[m/s]$	Poisson's ratio ν
1	50	2100	500	816.5	0.2
2	100	2300	750	1403.1	0.3
3	∞	2500	1000	2081.7	0.35

Substructure method is derived based on the principal of superposition, which could only indirectly model nonlinear problem via equivalent-linear approach (Solberg et al., 2016). It is noted that the formulation of DRM does not restrict the material behavior of interior soil. 3D inelastic constitutive behavior of soils under $3C$ seismic excitations can be considered using WP-DRM for realistic nonlinear SSI modeling (Wang et al., 2017, Sinha et al., 2017).

STRESS TEST OF SMALL MODULAR REACTOR (SMR)

The above WP-DRM has been implemented into high-fidelity finite element interpreter, Real-ESSI simulator (Jeremić et al., 1989-2019). Stress tests are performed for a deeply embedded SMR under $3C$ seismic motions from incident plane SV wave field. The finite element model of SMR is shown in Figure 1. The model is discretized by 152640 8-node brick elements. There are four layers of elements: SMR structure layer, inner soil layer, DRM layer and exterior absorbing layer. The length and width of the SMR structure is $30m$. The total height of the structure is $50m$ with $36m$ deeply embedded in the ground. The dimension of interior soil surrounding the structure is $150m \times 150m$ in horizontal directions and $60m$ in depth. Artificial viscous damping is applied at the exterior absorbing layer to absorb any outgoing wave and avoid the unrealistic boundary reflection of these waves.

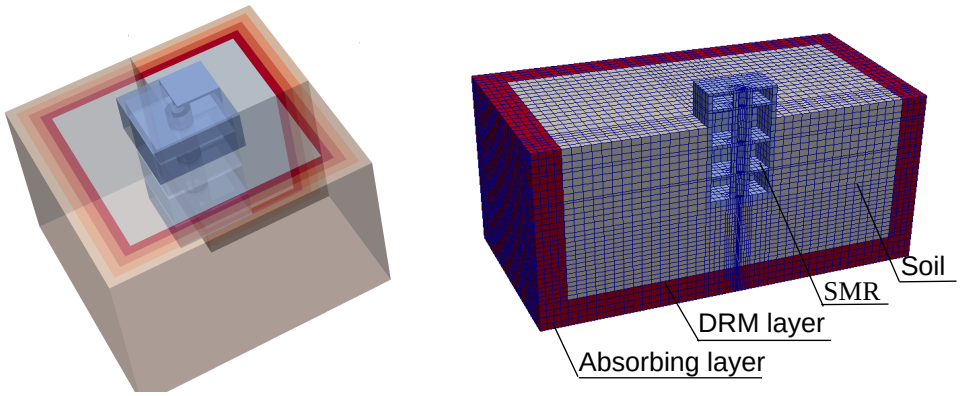

(a) Full FEM model (b) Half model section view

Figure 1: Illustration of FEM model of SMR

The properties of layering ground are given in table 1. The SSI system is stress tested with incident monochromatic SV waves from the bottom bedrock layer with different frequencies ($f = 1Hz, 2.5Hz, 5Hz$ and $10Hz$) and incident angles ($\theta = 10°, 45°, 60°$ and $80°$). The displacement magnitude of the incident SV wave from bedrock is kept the same as $0.065m$ for all cases.

Significantly different dynamic responses of SMR are shown in Figure 2 for incident SV wave with

different frequencies. In the case of $f = 1Hz$, the wavelength is very long. Dynamic SSI effects is not significant. SMR structure moves almost in the same pattern as free field motion. Along with the increase of frequency, the wave length becomes shorter and even comparable to the structural dimension in the case of $f = 10Hz$. Noticeably rocking response of SMR is observed. Furthermore, it can be seen that the existence of local structure significantly alter the near field seismic motions because of strong SSI.

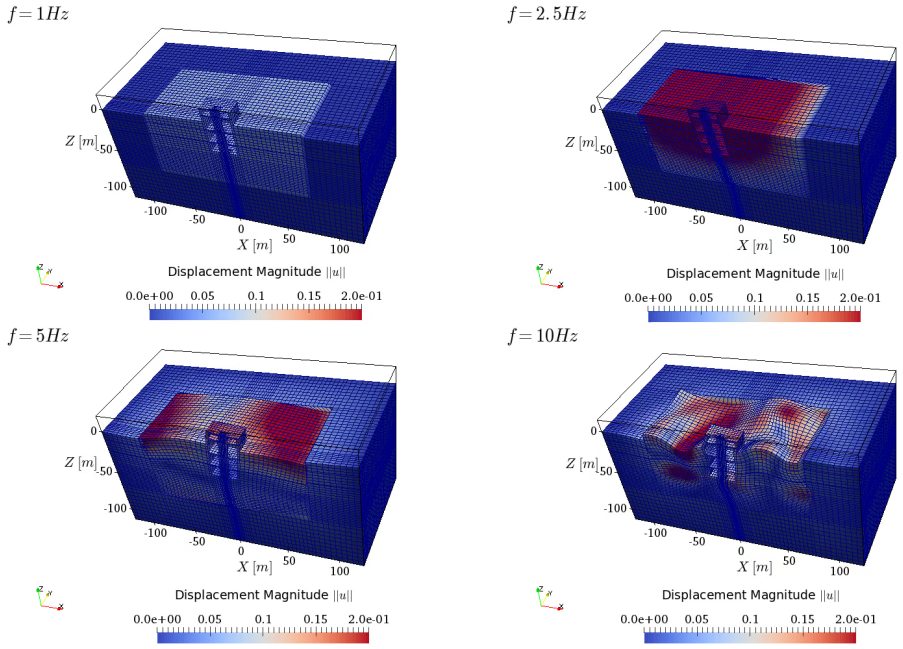

Figure 2: Dynamic response of SMR excited by stress test motions with incident angle $\theta = 60°$ and different frequencies

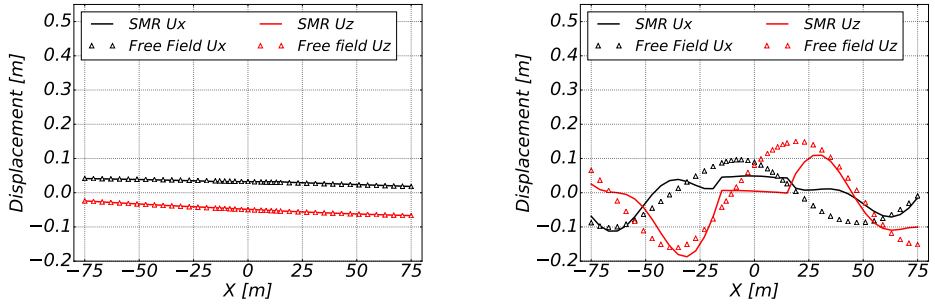

(a) $f = 1Hz$ (b) $f = 10Hz$

Figure 3: Spatial variation of displacement magnitude along the horizontal direction

Figure 3 compares the spatial variation of displacement magnitude of SMR along the horizontal direction with incident frequency $f = 1Hz$ and $f = 10Hz$. Compared with the case of $f = 1Hz$, the free field response given by $f = 10Hz$ is much larger and also shows larger spatial variation due to the short wavelength. Structural response of SMR is in good agreement with corresponding free field motion over the whole region with low frequency input $f = 1Hz$. However, for high frequency $3C$ motions $f = 10Hz$, "base averaging" of

displacement response in the region of SMR structure ($x \in [-15m, 15m]$) is clearly demonstrated in Figure 3(b). Because of the "base averaging", the structural displacement is smaller than corresponding free field motions. On the other hand, it is noted that the near field motion disturbed by SSI becomes larger, for example, the horizontal ground displacement in region ($x \in [25m, 50m]$) near SMR structure is greater than free field motions.

SMR is also stress tested using $3C$ motions from incident SV waves at different inclinations $\theta = 10°, 45°, 60°$ and $80°$. Corresponding deformation of SMR are compared in Figure 4. Significantly different displacement magnitudes of the structure can be seen: The displacement magnitude is the largest in the case of $\theta = 60°$ while the least in the case of $\theta = 80°$. Further comparisons reveal that different inclinations of incident SV wave mainly influence the vertical response of SMR.

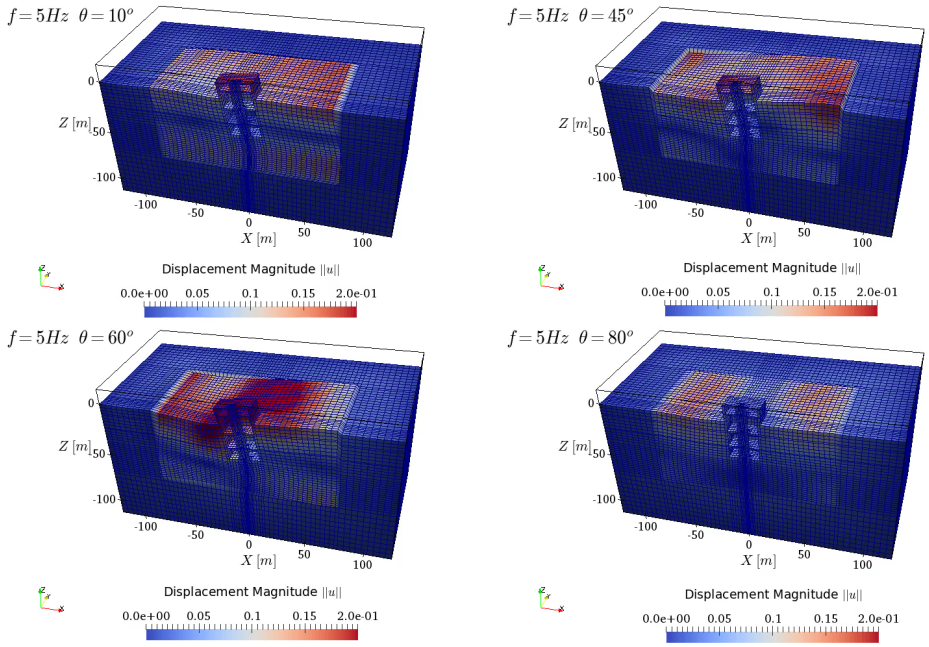

Figure 4: Dynamic response of SMR excited by stress test motions with frequency $f = 5Hz$ and different inclinations

Figure 5 shows dynamic response of top center of SMR structure in four different cases. Compared with free field motions, reduction in vertical displacement magnitude of the structure is seen in all the four cases. Among which, the largest reduction is experienced in the case of $\theta = 45°$, while the reduction is negligible when incident angle equals to $80°$. Furthermore, the phase shift in the dynamic response of SMR with respect to the free field motion is also noteworthy.

CONCLUSION

Spatially varying $3C$ seismic motions by oblique incident plane waves are solved with wave potential approach. Dynamic response of SSI system under $3C$ seismic excitations is modeled using wave potential - domain reduction method (WP-DRM). A deeply-embedded small modular reactor is stress tested with $3C$ seismic motions from incident SV wave with different frequencies and inclinations. Strikingly varying dynamic responses of SMR are obtained, which provide an estimation envelope and/or limit about the

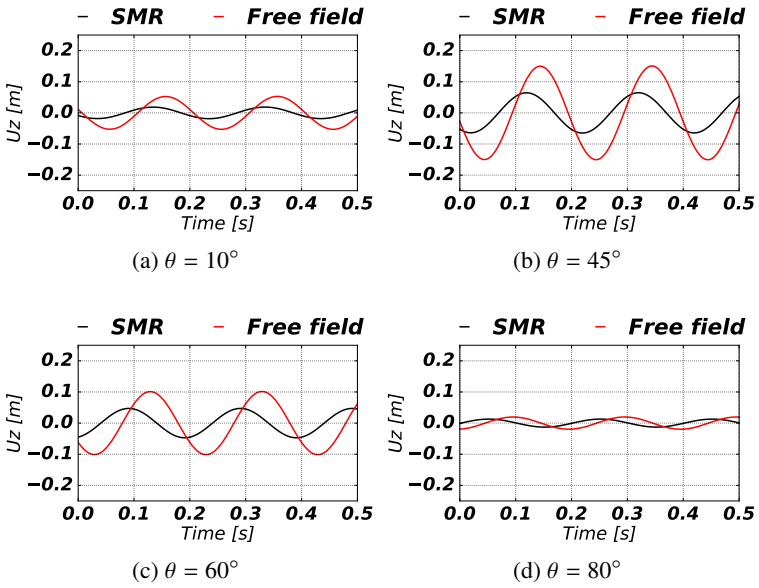

(a) $\theta = 10°$ (b) $\theta = 45°$

(c) $\theta = 60°$ (d) $\theta = 80°$

Figure 5: Vertical displacement response of top center of SMR under incident SV wave with frequency $f = 5Hz$ and different inclinations

structural dynamic response considering all the possible scenarios of seismic shaking. The high-frequency $3C$ excitations can cause significant SSI effects and structural rocking. More emphasis should be put on the properly modeling of dynamic response of NIs considering high frequency $3C$ motions. Attention should also be paid to the noticeable change (potential amplification) of near field motion when high frequency SV wave is incident to the SSI system of SMR. SMR is also stress tested with $3C$ seismic motions from incident SV wave at different angles of incidence. Vertical structural response is found to be highly dependent on the inclination angle of the incident SV wave. Incidence of SV wave at 45° results in the largest vertical structural deformation, while little vertical movement can be observed in the case of 80° incidence. Insights obtained from these stress tests can contribute to more economical and safe design of nuclear installations.

ACKNOWLEDGMENT

This work was supported in part by the US-DOE and UCD.

REFERENCES

Abell, J. A., Orbović, N., McCallen, D. B. & Jeremić, B. (2018), 'Earthquake soil structure interaction of nuclear power plants, differences in response to 3-D, 3×1-D, and 1-D excitations', *Earthquake Engineering and Structural Dynamics* **47**(6), 1478–1495.

Arfken, G. B. & Weber, H. J. (1999), *Mathematical methods for physicists*, AAPT.

Bielak, J., Loukakis, K., Hisada, Y. & Yoshimura, C. (2003), 'Domain reduction method for three–dimensional earthquake modeling in localized regions. part I: Theory', *Bulletin of the Seismological Society of America* **93**(2), 817–824.

Crouse, C. B., Hushmand, B., Luco, J. E. & Wong, H. L. (1990), 'Foundation impedance functions: Theory versus experiment', *Journal of Geotechnical Engineering* **116**(3), 432–449.

Cucci, L. & Tertulliani, A. (2011), 'Clues for a relation between rotational effects induced by the 2009 M_w 6.3

L'Aquila (central Italy) earthquake and site and source effects', *Bulletin of the Siesmological Society of America* **101**(3), 1109–1120.

Cucci, L. & Tertulliani, A. (2013), 'The earthquake-rotated objects induced by the 2012 Emilia (northern Italy) seismic sequence: Relation with seismological and geomorphological factors', *Seismological Research Letters* **84**(6), 973–981.

Fu, J., Liang, J. & Han, B. (2017), 'Impedance functions of three-dimensional rectangular foundations embedded in multi-layered half-space', *Soil Dynamics and Earthquake Engineering* **103**, 118–122.

Gičev, V., Trifunac, M. D. & Orbović, N. (2016), 'Two-dimensional translation, rocking, and waves in a building during soil-structure interaction excited by a plane earthquake P-wave pulse', *Soil Dynamics and Earthquake Engineering* **90**, 454 – 466.

Haskell, N. A. (1953), 'The dispersion of surface waves on multilayered media', *Bulletin of the seismological Society of America* **43**(1), 17–34.

Jeremić, B., Jie, G., Cheng, Z., Tafazzoli, N., Tasiopoulou, P., Pisanò, F., Abell, J. A., Watanabe, K., Feng, Y., Sinha, S. K., Behbehani, F., Yang, H. & Wang, H. (1989-2019), *The Real ESSI / MS ESSI Simulator System*, University of California, Davis and Lawrence Berkeley National Laboratory. `http://real-essi.info/`.

Jeremić, B., Jie, G., Preisig, M. & Tafazzoli, N. (2009), 'Time domain simulation of soil–foundation–structure interaction in non–uniform soils.', *Earthquake Engineering and Structural Dynamics* **38**(5), 699–718.

Jeremić, B., Tafazzoli, N., Ancheta, T., Orbović, N. & Blahoianu, A. (2013), 'Seismic behavior of NPP structures subjected to realistic 3d, inclined seismic motions, in variable layered soil/rock, on surface or embedded foundations', *Nuclear Engineering and Design* **265**, 85–94.

Kozák, J. T. (2009), 'Tutorial on earthquake rotational effects: Historical examples', *Bulletin of the Seismological Society of America* **99**(2B), 998–1010.

Liang, J., Fu, J., Todorovska, M. I. & Trifunac, M. D. (2013*a*), 'Effects of site dynamic characteristics on soil–structure interaction (ii): Incident p and SV waves', *Soil Dynamics and Earthquake Engineering* **51**, 58–76.

Liang, J., Fu, J., Todorovska, M. I. & Trifunac, M. D. (2013*b*), 'Effects of the site dynamic characteristics on soil-structure interaction (i): Incident SH-waves', *Soil Dynamics and Earthquake Engineering* **44**(0), 27 – 37.

Liang, J., Jin, L., Todorovska, M. I. & Trifunac, M. D. (2016), 'Soil-structure interaction for a SDOF oscillator supported by a flexible foundation embedded in a half-space: Closed-form solution for incident plane SH-waves', *Soil Dynamics and Earthquake Engineering* **90**, 287 – 298.

Luco, J. (1976), 'Torsional response of structures for sh waves: the case of hemispherical foundations', *Bulletin of the Seismological Society of America* **66**(1), 109–123.

Sinha, S. K., Feng, Y., Yang, H., Wang, H., Orbović, N., McCallen, D. B. & Jeremić, B. (2017), 3-d non-linear modeling and its effects in earthquake soil-structure interaction, *in* 'Proceedings of the 24th International Conference on Structural Mechanics in Reactor Technology (SMiRT 24)', Busan, South Korea.

Solberg, J. M., Hossain, Q. & Mseis, G. (2016), 'Nonlinear time-domain soil-structure interaction analysis of embedded reactor structures subjected to earthquake loads', *Nuclear Engineering and Design* **304**, 100 – 124.

Stress Test Peer Review Board (2012), Stress test performed on european nuclear power plants, Technical report, European Nuclear Safety Regulators Group (ENSREG).

Todorovska, M. & Trifunac, M. (1992), 'The system damping, the system frequency and the system response peak amplitudes during in-plane building-soil interaction', *Earthquake engineering & structural dynamics* **21**(2), 127–144.

Todorovska, M. I. (1993), 'Effects of the wave passage and the embedment depth for in-plane building-soil interaction', *Soil Dynamics and Earthquake Engineering* **12**(6), 343–355.

Trifunac, M., Ivanovć, S., Todorovska, M., Novikova, E. & Gladkov, A. (1999), 'Experimental evidence for flexibility of a building foundation supported by concrete friction piles', *Soil Dynamics and Earthquake Engineering* **18**(3), 169–187.

Wang, H., Yang, H., Feng, Y., Wang, F. & Jeremić, B. (2019), 'Wave potential-domain reduction method for 3D earthquake soil structure interaction', *to be submitted to: Soil Dynamics and Earthquake Engineering*. In review.

Wang, H., Yang, H., Sinha, S. K., Feng, Y., Luo, C., McCallen, D. B. & Jeremić, B. (2017), 3D non-linear earth-

quake soil-structure interaction modeling of embedded small modular reactor (SMR), *in* 'Proceedings of the 24th International Conference on Structural Mechanics in Reactor Technology (SMiRT 24)', Busan, South Korea.

Wolf, J. P. (1989), 'Soil-structure-interaction analysis in time domain', *Nuclear Engineering and Design* **111**(3), 381 – 393.

Wong, H. & Trifunac, M. (1974), 'Interaction of a shear wall with the soil for incident plane sh waves: elliptical rigid foundation', *Bulletin of the Seismological Society of America* **64**(6), 1825–1842.

Wong, L. H. & Luco, J. E. (1985), 'Tables of impedance functions for square foundations on layered media', *International Journal of Soil Dynamics and Earthquake Engineering* **4**(2), 64–81.

Yin, J., Nigbor, R. L., Chen, Q. & Steidl, J. (2016), 'Engineering analysis of measured rotational ground motions at GVDA', *Soil Dynamics and Earthquake Engineering* **87**, 125–137.

Yoshimura, C., Bielak, J. & Hisada, Y. (2003), 'Domain reduction method for three–dimensional earthquake modeling in localized regions. part II: Verification and examples', *Bulletin of the Seismological Society of America* **93**(2), 825–840.